

Deep-ocean soundscapes: The impact of atmospheric carbon dioxide

Gianluca Audone^{1,2}, Philippe Blondel³, Matthew Nunes⁴, and Chris Budd
OBE⁴

¹Dipartimento di Scienze Matematiche “Giuseppe Luigi Lagrange”,
Politecnico di Torino, Corso Duca degli Abruzzi, 24, 10129, Turin, Italy

²Gruppo Nazionale per il Calcolo Scientifico INdAM, Piazzale Aldo Moro 5,
00185, Rome, Italy

³Department of Physics, University of Bath, Bath, BA2 7AY, UK

⁴Department of Mathematical Sciences, University of Bath, Bath, BA2 7AY,
UK

Gianluca Audone, gianluca.audone@polito.it

Abstract: *The Comprehensive Nuclear Test Ban Treaty Organization manages a global International Monitoring System featuring 11 hydroacoustic stations installed in the deep-sea sound channel. Depending on when each station is commissioned, continuous measurements have accumulated up to 20 years of sound pressure data at frequencies reaching 100 Hz. These extended datasets provide a valuable foundation for exploring the long-term impacts of climate variability. This study uses data from CTBT stations Cape Leeuwin in the Indian Ocean and Wake Island in the Pacific Ocean, to investigate the impact of climate change on deep-ocean soundscapes. We analyse long-term acoustic data alongside atmospheric carbon dioxide (CO₂) concentration trends to understand their relationship. Continuous measurements from these stations provide a unique opportunity to assess climatic effects over extended periods. Multi-scale analysis of Sound Pressure Level (SPL) and Hjorth’s Mobility is used to correlate acoustic parameters with CO₂ concentrations. This approach allows us to detect seasonal changes and long-term climatic variations. Our findings reveal strong negative correlations between CO₂ trends and both SPL and Hjorth’s Mobility at Cape Leeuwin and Wake Island. The Intergovernmental Panel on Climate Change (IPCC) has highlighted the difficulty of gathering comprehensive long-term data to assess the impact of climate change in the deep sea (>1000 m). This research addresses this challenge by linking sound pressure levels at depth with atmospheric CO₂ concentrations. The observed relationships suggest that increasing CO₂ concentrations may be associated with decreasing sound levels and alterations in the frequency content of the underwater soundscape. Sound is an Essential Ocean Variable, and this study emphasises the importance of understanding the Earth’s climate system through deep-ocean acoustics.*

Keywords: *Deep-ocean acoustics, Sound Pressure Level, Atmospheric CO₂ coupling, CTBTO IMS hydrophones, Low-frequency absorption*

1. INTRODUCTION

Sound is the primary carrier of information in the sea. Marine mammals, fish, and invertebrates depend on it for communication, navigation, and foraging, while human activities, such as shipping, the extraction of seabed resources and sonar, continuously shape the ambient soundscape [1, 2]. Detecting climate-driven changes within this noisy environment is therefore essential to both safeguarding the ecosystem and regulating anthropogenic actions.

The Intergovernmental Panel on Climate Change (IPCC) reported that warming has been strongest so far in the upper 0–700 m of the ocean; quantifying trends below 1,000 m remains notoriously difficult because sustained observations are sparse [3]. However, the deep-sea sound channel (SOFAR) offers an acoustic window into this blind spot. Because the speed of the sound is coupled to temperature, salinity, and pressure, even subtle hydrographic changes can imprint detectable changes on the propagation of low frequency [1]. Moreover, increasing atmospheric CO₂ alters seawater absorption, reducing attenuation below 100 Hz and potentially lowering ambient Sound Pressure Level (SPL) while reshaping the spectra [4]. Ainslie showed that seasonal Sea Surface Temperature (SST) variability can modulate acoustic levels at mid-latitudes [6]; however, direct long-term links between deep-ocean acoustics and atmospheric climate drivers remain largely unexplored because suitable records are scarce.

The global hydroacoustic network of the Comprehensive Nuclear-Test-Ban Treaty Organization (CTBTO) with its eleven IMS stations, deployed in the SOFAR channel and operating quasi-continuously since the early 2000s, now holds up to two decades of broadband data (up to 100 Hz) [7]. In this study we exploit two stations that span contrasting oceanographic regimes: **Cape Leeuwin (HA01)**, a temperate, mid-latitude site sensitive to the Leeuwin Current and Southern Ocean variability, and **Wake Island (HA11)**, a tropical North Pacific site influenced by pronounced seasonal cycles and the El Niño–Southern Oscillation (ENSO).

Our objectives are to:

1. quantify correlations between multiscale acoustic metrics and globally averaged atmospheric CO₂ concentrations from 2004–2023;
2. assess whether geographically distant basins share coherent acoustic responses that may constitute a global fingerprint of climate change.

2. DATA PROCESSING

Acoustic waveforms from CTBTO hydroacoustic stations are sampled at 250 Hz with 24-bit resolution, providing usable frequency content up to 100 Hz with a theoretical dynamic range of 144 dB. Each daily file is accompanied by metadata specifying per-channel sensitivity and gain coefficients; raw analogue-to-digital counts are converted to instantaneous sound pressure by applying these coefficients and the manufacturer-supplied hydrophone inverse response [8]. The resulting pressure series is high-pass filtered at 1 Hz to remove hydrostatic offsets.

Calibrated data are segmented into contiguous 60-s records ($N = 15,000$ samples), tapered with a Hann window to reduce spectral leakage, and transformed to the frequency domain using the Fast Fourier Transform (FFT). One-Third-octave band power spectral densities are then computed according to ANSI S1.11-2014 [5]; bands with centre frequencies from 1.12 to 100

Hz are retained. The broadband Sound Pressure Level (SPL) is obtained by

$$\text{SPL} = 10 \log_{10} \left(\sum_k P_k \right) \quad \text{dB re } 1 \mu\text{Pa}^2 \quad (1)$$

where P_k denotes the mean-squared sound pressure in the k^{th} one-third octave band.

Hjorth's Mobility denoted by \mathcal{M} is computed as a spectral-moment proxy for mean frequency. Although originally formulated in the time domain, Mobility can be expressed through spectral moments via Parseval's theorem. Let $\hat{p}(f_k)$ be the FFT of a 60-s window and σ_n^2 the variance of the n^{th} temporal derivative; then

$$\mathcal{M} = \sqrt{\sigma_2^2 / \sigma_0^2}, \quad (2)$$

where

$$\sigma_0^2 = \sum_k |\hat{p}(f_k)|^2, \quad \sigma_2^2 = \sum_k \omega_k^2 |\hat{p}(f_k)|^2$$

with $\omega_k = 2\pi f_k$. Equations (2) make clear that both SPL and Mobility are derived consistently from the calibrated frequency spectrum, ensuring comparability with other studies [11, 12]. The 1-min metrics are then averaged to weekly means, the cadence used throughout the correlation analyses. Weekly aggregation suppresses short impulsive events while retaining intra-annual variability.

Atmospheric CO₂ concentrations are taken from the weekly Global Greenhouse Gas Reference Network product of NOAA's Mauna Loa Observatory¹.

3. METHODOLOGY

The analysis follows these three successive stages —spectral exploration, multi-scale decomposition, and lag-resolved correlation— applied independently to the four one-third-octave bands that visual inspection showed to be most informative: band 13 (19.9 Hz), band 14 (25.1 Hz), band 19 (63.1 Hz) and band 20 (79.4 Hz). Centre frequencies follow the ANSI S1.11 definitions [5].

Spectral exploration. The spectrogram analysis revealed (i) a persistent baleen-whale chorus near 20 Hz, (ii) a broad attenuation feature between 60 Hz and 80 Hz, and (iii) an absence of long-lived instrumental tones. These observations motivated restricting out analyses to the four bands listed above. Figure 1 shows representative spectrograms for each station.

Time-series decomposition. Each acoustic series is decomposed using Seasonal–Trend decomposition with LOESS (STL) [9]. Let $y_{b,t}$ denote either SPL or \mathcal{M} in band b during week t ; STL represents

$$y_{b,t} = T_{b,t} + S_{b,t} + R_{b,t},$$

where $T_{b,t}$ is the long-term trend, $S_{b,t}$ is the seasonal component, and $R_{b,t}$ is the remainder. The same procedure is applied to the weekly atmospheric CO₂ record from Mauna Loa, yielding directly comparable trend and seasonal sub-series. Residual autocorrelation and quantile-quantile (Q-Q) plots confirmed that seasonality had been adequately removed.

¹<https://gml.noaa.gov/ccgg/trends/mlo.html>

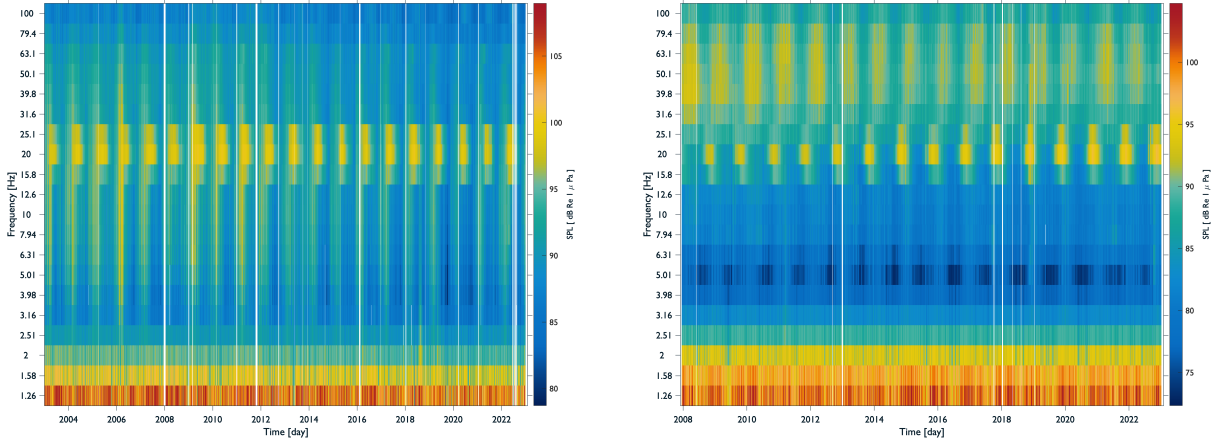


Figure 1: Daily Welch spectrograms for Cape Leeuwin (left) and Wake Island (right). Persistent energy near 20 Hz corresponds to baleen-whale calling, while a basin-scale attenuation feature is visible around 60–80 Hz.

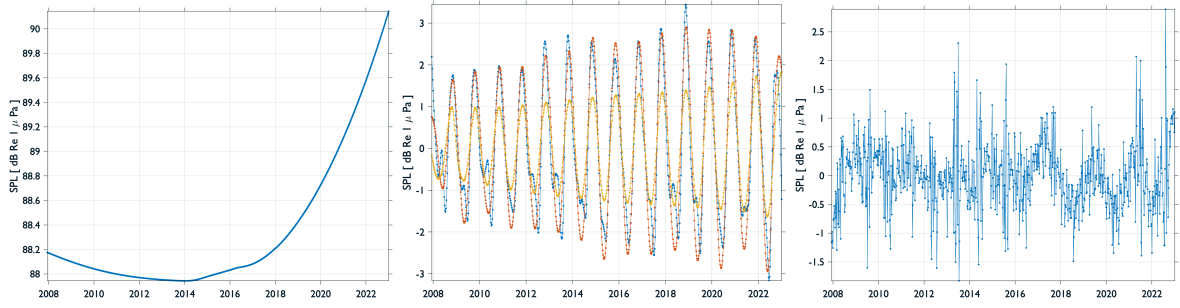


Figure 2: STL decomposition of weekly SPL at Wake Island, band 13. Left to right: long-term trend $T_{13,t}$, seasonal component $S_{13,t}$ (52-week period), and remainder $R_{13,t}$.

Correlation analysis. Long-term associations are quantified with the Pearson product moment coefficient $r(\ell)$ between the trend component of each acoustic metric and the trend in atmospheric CO_2 . Phase alignment within the annual cycle is examined by finding the lag that maximises the absolute Pearson correlation between the seasonal components of the acoustic series and the CO_2 record.

This integrated workflow—targeted spectral filtering, STL separation and lag-resolved correlation—provides a compact yet comprehensive basis for detecting and attributing CO_2 -driven fingerprints in the deep-ocean acoustic environment while rigorously controlling for seasonality and autocorrelation.

4. ANALYSIS

The weekly time series of Sound Pressure Level (SPL) and Hjorth’s Mobility, \mathcal{M} , are examined in the four diagnostic one-third-octave bands—13 (19.9 Hz), 14 (25.1 Hz), 19 (79.4 Hz) and 20 (100 Hz), where the numbers in parentheses are the centre frequencies of each band. The analysis follows the procedure set out in Sec. 3. To investigate the statistical significance of the trends we fitted a linear and a quadratic model.

At Cape Leeuwin the decline in SPL is coherent across every frequency considered. Specifically, in band 13, the SPL decreases by $0.15 \text{ dB re } 1 \text{ dB re } 1 \mu\text{Pa}^2$ per year. In band 14, the

decrease is 0.14 dB re 1 dB re $1 \mu\text{Pa}^2$ per year. Band 19 experiences a decrease of 0.22 dB re 1 dB re $1 \mu\text{Pa}^2$ per year, and band 20 shows a decrease of 0.16 dB re 1 dB re $1 \mu\text{Pa}^2$, see Figure 3. These findings indicate a consistent downward trend in SPL across all examined bands. The p-value is equal to zero for all bands. Quadratic models showed no improvements over the linear ones.

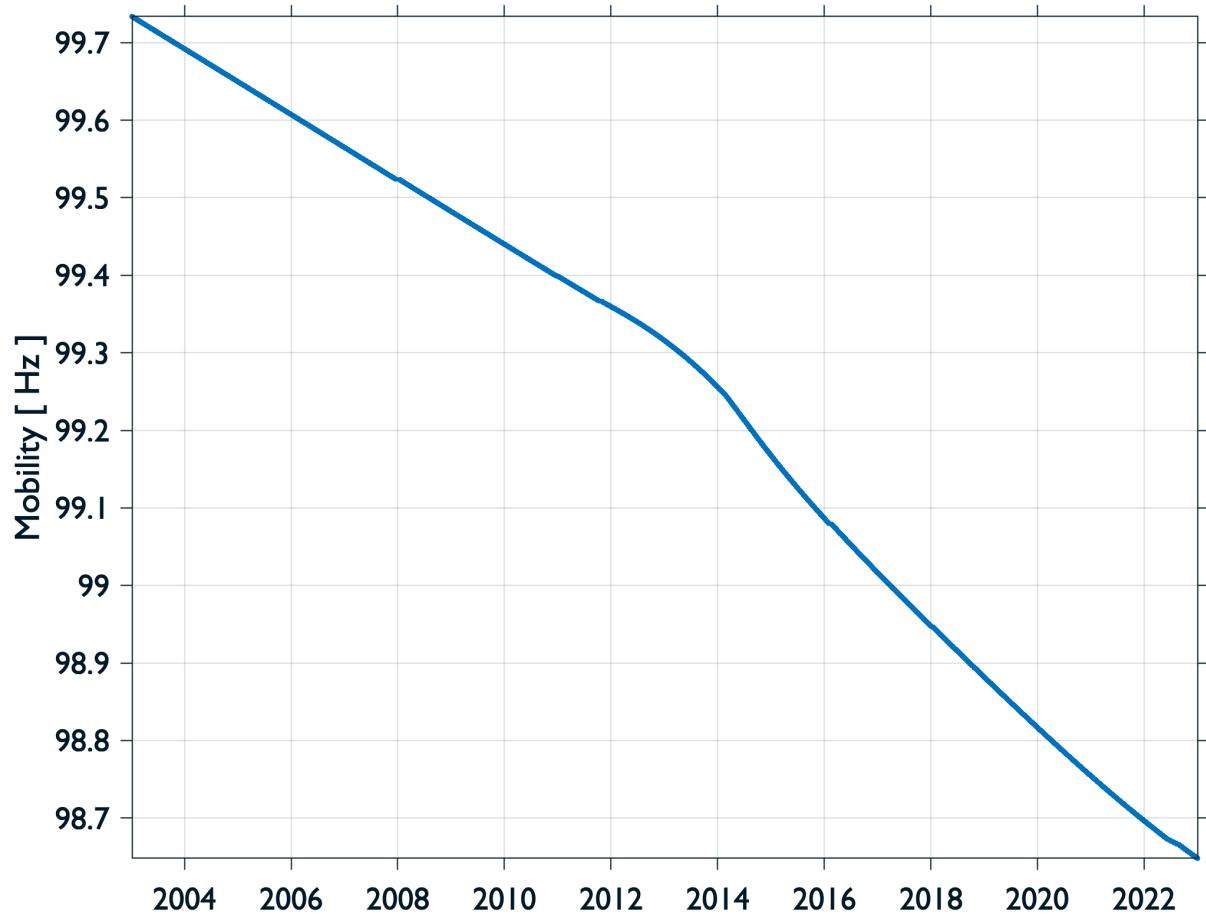


Figure 3: Long-term trend in Hjorth's Mobility band 20 (centre 100 Hz) at Cape Leeuwin (H01W1). This figure displays the trend in Hjorth's Mobility for band 20 at Cape Leeuwin. We point out the strong linear decrease of 1 Hz. This trend provide insights into the long-term evolution variability of underwater sound at this location.

Hjorth's mobility shows a decrease by 0.0017 Hz per year in band 13, while bands 14 shows a decrease of 0.0198 Hz per year. We see an increase of 0.0152 Hz per year in band 19, and a decrease by 0.0572 Hz per year in band 20. These results highlight distinct trends in mobility across different bands, with some bands showing an increase and others a decrease over time. In this case quadratic models gave slightly better fit than the linear models, particularly for bands 13 and 19. This suggests a non-linear relationship in mobility to be explored.

Wake Island Sound Pressure Level trends for bands 13 and 14 are best described by a quadratic model while bands 19 and 20 need more complex model for the trend. A linear model is fitted to have an estimate of the trend. Band 13, the SPL decreases by 0.09 dB re $1 \mu\text{Pa}^2$ per year. Band 19 experiences a decrease of 0.06 dB re $1 \mu\text{Pa}^2$ per year, and band 20 shows a decrease of 0.06 dB re $1 \mu\text{Pa}^2$ per year. These findings indicate a consistent downward trend in SPL across these examined bands. For band 14, the linear model shows a statistically significant increase in SPL over time with a p-value of 0.00016, with an increase of 0.01 dB re $1 \mu\text{Pa}^2$ per year.

Hjorth's mobility bands 13 is best described by a linear model and we see an increase of 0.0102 Hz per year. All the other bands do not show significant changes to model the trend.

Lag-resolved correlation To quantify the link with atmospheric carbon loading, Pearson coefficients between the acoustic trends and the Mauna Loa CO₂ trend are evaluated. At Cape Leeuwin, SPL shows consistent strong negative correlations across all bands ranging from -0.84 to -0.94 . Band 20 is the only to present a lag effect with 2 and a half months. Mobility's trends only shows negative strong correlations (-0.9) for bands 14 and 20 and strong positive correlation (0.96) for band 19. There is no lag effect.

Wake Island shows no lag for both SPL and Mobility. SPL band 13 has correlation of 0.7 while band 14 show -0.7 correlation. Band 20 has -0.9 correlation. Mobility's band 13 has correlation of 0.9, band 14 correlation of -0.8 , band 19 of 0.5 and lastly band 20 with 0.3.

Seasonal variability SPL at Cape Leeuwin shows for band 13 and 14 a positive cross correlation of 0.88 between two to three weeks. Bands 19 and 20 show respectively negative and positive correlation with an absolute value of 0.5 at five and two month respectively. Mobility has strong negative correlation -0.8 for band 13 with 3 months lag. Band 20 show negative correlation -0.6 with a month lag, band 19 a weaker positive correlation of 0.47 at 5 month lag. Mobility's band 14 show no correlation.

Wake Island SPL show negative correlation -0.91 with a month lag for band 13, -0.83 with two and a half month lag for band 14 and bands 19 and 20 with -0.77 with four and a half months lag. Mobility has correlation of 0.86 with no lag for band 13, we find the same correlation for band 14 with a lag of one month and a half. Weak correlation -0.3 is found for bands 19 and 20.

5. CONCLUSIONS AND FUTURE WORK

Weekly records from the Cape Leeuwin and Wake Island IMS hydrophones provide a first view of how the deep-ocean acoustic environment may be evolving in a period of rapidly rising atmospheric CO₂. At both sites the 20-year trend in low-frequency (< 100 Hz) Sound Pressure Level is downward, with fitted slopes of roughly -0.2 dB yr⁻¹ at Cape Leeuwin and -0.1 dB yr⁻¹ at Wake Island, although one biologically dominated band at the latter shows a small increase. Hjorth's Mobility, a proxy for mean spectral frequency, changes in a broadly consistent manner, but its band-to-band diversity cautions that source composition and local conditions also play a role. Correlations with the Mauna Loa CO₂ record are negative and peak at lags close to zero weeks, behaviour that is qualitatively consistent with higher carbon concentrations but that cannot, on its own, exclude alternative explanations such as basin-scale variations in shipping, baleen-whale population dynamics, or instrumentation biases.

No systematic change is detected above about 50 Hz, in line with theory that predicts chemically mediated absorption to be strongest below 100 Hz. Even so, the data originate from only two stations, and their interpretation is complicated by uncertainties in long-term sensor calibration, by incomplete knowledge of regional source statistics and by the possibility of subtle environmental influences (e.g. mesoscale circulation) that fall outside the present analysis framework.

Several extensions could therefore help to clarify the emerging picture. Repeating the band-resolved workflow at the remaining IMS hydrophones—and at other observatories with decade-scale coverage—would test whether the Cape–Wake behaviour is regionally confined or part

of a larger-scale pattern. Combining acoustic records with ship-tracking data, earthquake catalogues and modern source-separation techniques should allow a more explicit attribution of the long-term level change to anthropogenic, geophysical and biological components. Parallel work linking low-frequency trends to independent observations of marine fauna—whether passive-acoustic call detections, fisheries statistics—could shed light on ecological consequences. Finally, embedding calibrated SPL and Mobility diagnostics in coupled ocean – acoustic – biogeochemical models will be essential if deep-ocean sound is to become a quantitative indicator of carbon-cycle change.

Viewed in that context, hydroacoustic archives represent a largely untapped but promising complement to physical and chemical oceanographic datasets.

6. ACKNOWLEDGEMENTS

GA acknowledges the support of the Fondazione Compagnia di San Paolo within the framework of the Artificial Intelligence Call for Proposals, Alxtreme project (ID Rol: 71708). GA was supported by a PhD studentship from the Engineering and Physical Sciences Research Council (EPSRC, UK) to the University of Bath's Centre for Doctoral Training in Statistical Applied Mathematics at Bath (SAMBa), project #EP/L015684/1m, and by the National Physical Laboratory. GA acknowledges the support of V. Livina (NPL) in downloading and organizing the data, and S.-H. Cheong (NPL) in the initial data processing. The views expressed in the paper are those of the authors and do not necessarily represent those of the CTBTO.

REFERENCES

- [1] Woolfe, K. F., Lani, S., Sabra, K. G., and Kuperman, W. A.: “Monitoring deep-ocean temperatures using acoustic ambient noise: passive acoustic tomography in the ocean”, *Geophys. Res. Lett.* **42**, 2878–2884 (2015).
- [2] Ainslie, M. A. and McCole, J. G.: “A simplified formula for viscous and chemical absorption in sea water”, *J. Acoust. Soc. Am.* **103**, 1671–1672 (1998).
- [3] Barros, V. R. *et al.*, *Climate Change 2014: Impacts, Adaptation, and Vulnerability*, Contribution of WG II to the Fifth Assessment Report of the IPCC (Cambridge University Press, 2014).
- [4] Reeder, D. B. and Chiu, C. S.: “Ocean acidification and its impact on ocean noise: phenomenology and analysis”, *J. Acoust. Soc. Am.* **128**, EL137–EL143 (2010).
- [5] ANSI/ASA S1.11-2014: “Specification for octave-band and fractional-octave-band analog and digital filters” (Acoustical Society of America, New York, 2014).
- [6] Ainslie, M. A., Andrew, R. K., Howe, B. M., and Mercer, J. A.: “Temperature-driven seasonal and longer-term changes in basin-averaged deep-ocean ambient sound at 63–125 Hz”, *J. Acoust. Soc. Am.* **149**, 2531–2545 (2021).
- [7] Prior, M., Brown, D., Haralabus, G., and Stanley, J.: “Long-term monitoring of ambient noise at CTBTO hydrophone stations”, in *Proc. 11th European Conf. on Underwater Acoustics* (Edinburgh, 2012).

- [8] Robinson, S. P., Lepper, P. A., and Hazelwood, R. A.: *Good Practice Guide for Underwater Noise Measurement*. National Measurement Office, Marine Scotland, and The Crown Estate. NPL Good Practice Guide No. 133, ISSN 1368–6550, 2014.
- [9] Cleveland, R. B., Cleveland, W. S., McRae, J. E., and Terpenning, I.: “STL: a seasonal-trend decomposition procedure based on LOESS”, *J. Off. Stat.* **6**, 3–73 (1990).
- [10] Brockwell, P. J. and Davis, R. A., *Time Series: Theory and Methods*, 2nd ed. (Springer, 1991).
- [11] Hjorth, B.: “EEG analysis based on time-domain properties”, *Electroencephalogr. Clin. Neurophysiol.* **29**, 306–310 (1970).
- [12] Hjorth, B.: “The physical significance of time-domain descriptors in EEG analysis”, *Electroencephalogr. Clin. Neurophysiol.* **34**, 321–325 (1973).